



CHAPTER II

THEORY AND LITERATURE REVIEWS

2.1 Gas separation by adsorption process

Separation may be defined as a process that transforms a mixture of substances into two or more products that differ from each other in composition. The process is difficult to achieve because it is the opposite of mixing, a process favored by the second law of thermodynamics. Consequently, the separation steps often account for the major production costs in chemical and petrochemical industries. Separation also plays a key role in chemistry and related scientific disciplines. Through the endeavor of human ingenuity, there exist a multitude of industrial separation processes and laboratory separation techniques [6].

The surface of a solid represents a discontinuity of its structure. The forces acting at the surface are unsaturated. Hence, when the solid is exposed to a gas, the gas molecules will form bonds with it and become attached. This phenomenon is termed adsorption.

Adsorptive gas separation processes can be divided into two types: bulk separation and purification. The former involves adsorption of a significant fraction, 10% by weight or more according to Keller's definition, from a gas stream, whereas in purification less than 10% by weight of a gas stream to be adsorbed. Such a differentiation is useful because, in general, different process cycles are used for different types of separation.

Purification includes: drying (or dehydration) of air, natural gas, olefin-containing cracked gas, synthesis gas and other industrial gases; hydrogen purification; sweetening (removal of acid gases) of natural gas and plant-separation processes are the production of oxygen and nitrogen from air, separation processes are the production of oxygen and nitrogen from air, separation of n-paraffins from iso-paraffins and aromatics, and hydrogen from industrial gases. Molecular-sieve zeolites and activated carbon are the major sorbents used. However, the molecular-sieving property is not used in most of the commercial processes where zeolites are used. The separation is based on differences in equilibrium isotherms, and the slow intracrystalline diffusion is actually detrimental to



separation. The molecular-sieving property is used in only three known commercial processes:

- a) n- and iso-paraffin separation using 5A zeolite
- b) Drying of various gas streams using zeolites
- c) Nitrogen production from air using molecular-sieve carbon

The two former separations are accomplished based on selective molecular exclusion, whereas the latter is the only process using differences in pore diffusivity.

Fixed-bed adsorbers are used in almost all known commercial processes with the exception of the Purasiv HR process. For continuous feed and products, dual-bed or multibed systems are used in which each bed goes through adsorption regeneration cycles. Although the operation of each bed is batchwise, the system as whole is a continuous one that is operated in a cyclic steady state. Based on the method of sorbent regeneration and the mechanical arrangement, a number of process cycles and combinations of cycles have been developed. They are:

- a) Thermal-swing adsorption: In this process cycle, the bed is regenerated by raising the temperature. The most convenient way of raising the temperature is by purging the bed with a preheated gas. This is the oldest and most completely developed adsorption cycle. Because heating is a slow and often rate-limiting step, the length of each cycle usually ranges from several hours to over a day. In order to make the time length of the adsorption step comparable to that of regeneration, the cycle is used only for purification purposes.
- b) Pressure-swing adsorption: In this cycle the bed regeneration is accomplished by reducing the total pressure. The cycle time is short, usually in minutes or even seconds, due to the possibility of rapid pressure reduction. Though ideally suited for bulk separations, this cycle can be used for purifications as well. An increasing number of purification processes are being switched from temperature swing to this cycle, and an increasing number of bulk separation processes are being developed using this cycle. This is the youngest basic cycle and also the

most flexible one in terms of process modification. Unlike the temperature-swing and other cycles, many new applications are possible with the pressure-swing cycle. This cycle is also the most difficult and complex to model.

- c) Inert purge: This cycle is similar to the temperature-swing cycle except that preheating of the purge gas is not required. Usually a fraction of the light product (raffinate) is used as the inert purge gas.
- d) Gas chromatography: The laboratory analytical chromatography has been an appealing tool for large-scale separation for many years. Only recently have commercial attempts appeared successful
- e) Parametric pumping and cycling-zone adsorption: These two processes have yet to find a commercial application. Nevertheless, there are still ongoing research activities, and future applications are not out of the question.
- f) Moving-bed and simulated moving-bed processes: In these processes the gas mixture and solid sorbent are contacted in a countercurrent movement. Thus, unlike the temperature- and pressure-swing processes, the process is truly steady state in that the flow rates and compositions of all streams entering and leaving the adsorbent bed are constant. Besides the process simplicity, a further advantage of the moving-bed process is in minimizing the required inventory of adsorbent.

This research studies the condition and adsorbent that are suitable for hydrogen purification by adsorption process which purifies hydrogen by adsorbing impurities molecules on a very porous material like molecular sieve which is cooled by a cryogen, typically liquid nitrogen. The main advantages are simple process, low pressure drop for light product.

Construction and Operation

This process employs compressors to control the feed gas (hydrogen, HP industrial grade 99.99%) to an acceptable pressure. The feed gas was pre-treated by silica gel before passing the 2 columns made from stainless steel filled with alumina and zeolite dipped in liquid nitrogen bath. Gases will now either condense or be adsorbed by the large surface of the molecular sieve. Then the purified gas will pass the water bath to adjust the temperature before filling into the cylinders as ultra high purity hydrogen (99.999%).

In the regeneration, the molecular sieves are heated to 300 °C for zeolite and 180°C for alumina to drive off guest molecules accumulate in the molecular sieve. It takes typically 3 hours to fully regenerate.

2.2 Industrial sorbents

In principle, all microporous materials can be used as sorbents for gas purification and separation. For example, bone chars, coal chars, calcined clays, iron oxide, calcined bauxite, and the like have all found commercial uses. The four sorbents to be discussed here, however, are those with well-controlled and high microporosity, and are produced in large quantities. Table 2.1 provides a perspective of the relative amounts used and the major gas separations performed in industry. In addition to developed since about the mid-1970s, will also be discussed because of its unique ability to perform kinetic separation based on the different pore diffusion rates of different gas molecules.

Table 2.1 Application and annual productions of major industrial sorbents.

Sorbent	Annual U.S. production ^a	Major uses for gas sorption
2.1.1 Activated carbon	90,000 (major)	Removal of nonpolar gases and organic vapors (e.g., solvents, gasoline vapor, odors, toxic and radioactive gases); H ₂ purification; etc.
2.2.2 Zeolites:		
Synthetic	30,000b (major)	Drying; H ₂ purification; air purification; air separation; separations based on molecular size and shap (e.g., n- and iso-paraffins, aromatics, etc.); gas chromatography
Natural	250,000b (minor)	
2.2.3 Silica gel	150,000 (minor)	Drying; gas chromatography
2.2.4 Activated alumina	25,000 (major)	Drying; gas chromatography

a Late 1970s figure in metric tons. The fraction used as sorbent is indicated in parentheses.

b Worldwide total figure.

2.2.1 Activated Carbon

Manufacturing Processes

The manufacture and use of activated carbon date back to the nineteenth century. The modern manufacturing processes basically involve the following steps: raw material preparation, palletizing, low-temperature carbonization, and activation. The conditions are carefully controlled to achieve the desired pore structure and mechanical strength.

The raw materials for activated carbon are carbonaceous matters such as wood, peat, coals, petroleum coke, bones, coconut shell, and fruit nuts. Anthracite and bituminous coals have been the major sources. Starting with the initial pores present in the raw material, more pores, with desired size distributions, are created by the so-called activation process. After initial treatment and palletizing, one activation process involves carbonization at 400-500°C to eliminate the bulk of the volatile matter, and then partial

gasification at 800-1,000°C to develop the porosity and surface area. A mild oxidizing gas such as CO₂, steam, or flue gas is used in the gasification step because the intrinsic surface reaction rate is much slower than the pore diffusion rate, thereby assuring the uniform development of pores throughout the pellet. The activation process is usually carried out in fixed beds, but in recent years fluidized beds have also been used. The activated carbon created by this activation process is used primarily for gas and vapor adsorption processes. The other activation process that is used commercially depends on the action of inorganic additives to degrade and dehydrate the cellulosic materials and, simultaneously, to prevent shrinkage during carbonization. Lignin, usually the raw material that is blended with activators such as phosphoric acid, zinc chloride, potassium sulfide, or potassium thiocyanate, is carbonized at temperatures up to 900°C. The product, usually in powder form, is used for aqueous or gas purposes. The inorganic material contained in activated carbon is measured as ash content, generally in the range between 2 and 10%.

Surface Properties for Adsorption

The unique surface property of activated carbon, in contrast to the other major sorbents, is that its surface is nonpolar or only slightly polar as a result of the surface oxide groups and inorganic impurities. This unique property gives activated carbon the following advantages:

- a) It is the only commercial sorbent used to perform separation and purification processes without requiring prior stringent moisture removal, such as is needed in air purification. (It is also useful in aqueous processes.)
- b) Because of its large accessible internal surface, it adsorbs more nonpolar and weakly polar organic molecules than other sorbents do. For example, the amount of methane adsorbed by activated carbon at 1 atmosphere (atm) and room temperature is approximately twice that adsorbed by an equal weight of molecular sieve 5A (Figure 2.1)

- c) The heat of adsorption, or bond strength, is generally lower on activated carbon than on other sorbents. Consequently, stripping of the adsorbed molecules is easier and results in lower energy requirements for regeneration of the sorbent.

It is not correct, however, to regard activated carbon as hydrophobic. The equilibrium sorption of water vapor on an anthracite-derived activated carbon is compared with that of other sorbents in Figure 2.2. The sorption of water vapor on activated carbon follows a Type V isotherm (according to the BDDT classification) due to pore filling or capillary condensation in the micropores. Activated carbon is used, nonetheless, in processes dealing with humid gas mixtures and water solution because the organic and nonpolar or weakly polar compounds adsorb more strongly, and hence preferentially, on its surface than water does.

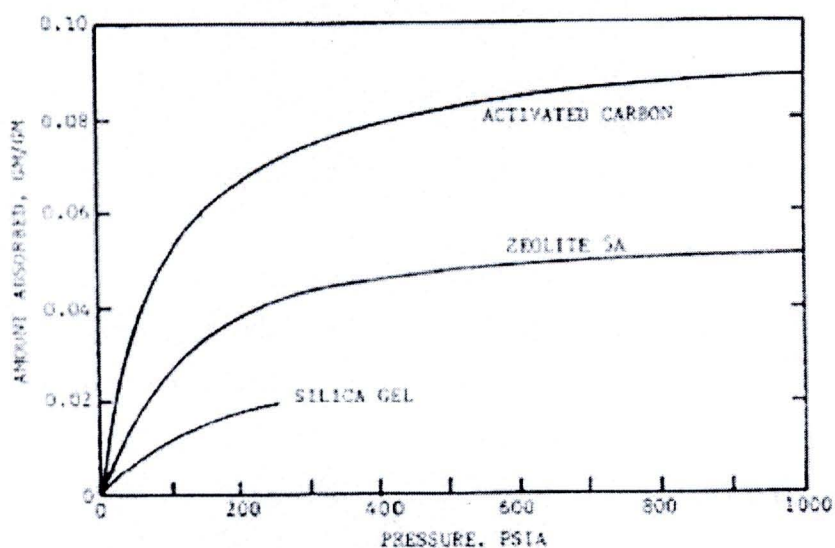


Figure 2.1 Equilibrium sorption of methane at 25°C on silica gel, zeolite 5A, and activated carbon.

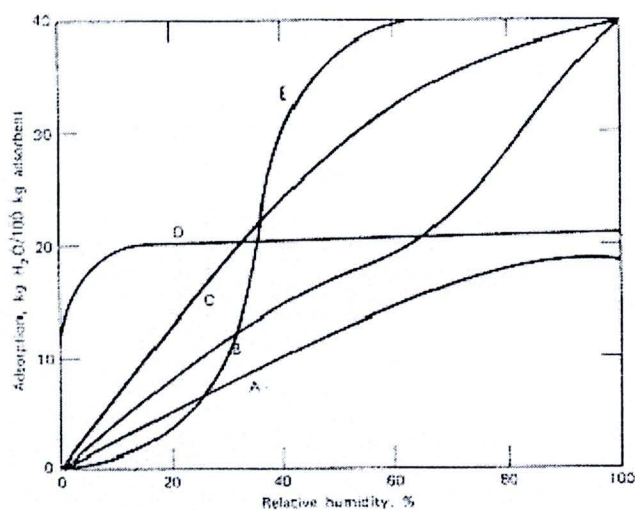


Figure 2.2 Equilibrium sorption of water vapor from atmospheric air at 25°C on (A) alumina (granular); (B) alumina (spherical); (C) silica gel; (D) 5A zeolite; (E) activated carbon. The vapor pressure at 100% R.H. is 23.6 Torr.

Attempts have been made to modify the surface of activated carbon chemically for special applications. However, successful commercial operations have been limited to liquid-phase applications. In gas-phase applications, it has been shown that by increasing the polarity of the surface, the amount of water vapor adsorbed at low relative pressures (below 4 Torr at 25°C; see Figure 2.2) can be drastically increased. For example, Walker and co-workers showed a hundred fold increase in water vapor adsorption by activated carbon after surface oxidation by HNO_3 . Exchange of the surface H-ions by cations (Li, Na, K, Ca) on the oxidized carbon further increased the moisture capacity at low vapor pressures to amounts comparable to that on zeolites. The ion-exchanged carbon was fully regenerated at 140°C, in contrast to temperatures over 350°C required for zeolite regeneration.

Pore Structure of Activated Carbon

Activated carbons are characterized by a large surface area between 300 and 2,500 m^2/g , as measured by the BET method, which is the largest among all sorbents. Commercial grades of activated carbon are designated for either gas phase or liquid phase of adsorbates, depending on its application. A majority of the pore volume is near or

larger than 30 Å in diameter in carbons for liquid phase adsorbate, whereas the pores of carbons for gas-phase adsorbate are mostly in the range from 10 Å to 25 Å in diameter. Carbons for liquid phase adsorbate need large pores because of the large size of many dissolved adsorbates, and the slower diffusion in liquid than in gas for the same size molecules.

A polymodal pore-size distribution is generally found in activated carbon. The pore structure may be pictured as having many small pores branching off from large ones, which are open through the entire particle. The large pores are called feeder or transport pores; the smaller ones, which may be dead-end, are called adsorption pores. According to the International Union of Pure and Applied Chemistry (IUPAC) classification, the pores are subdivided by diameter (d) into macropores ($d > 500$ Å), mesopores (20 Å $< d < 500$ Å), and micropores ($d < 20$ Å). The cumulative pore-volume distribution of the fine pores for a typical gas-phase activated carbon is shown, along with four other sorbents, in Figure 2.3. The larger pores are mostly submicron in size, and their total volume amounts to a fraction of that found in the fine pores.

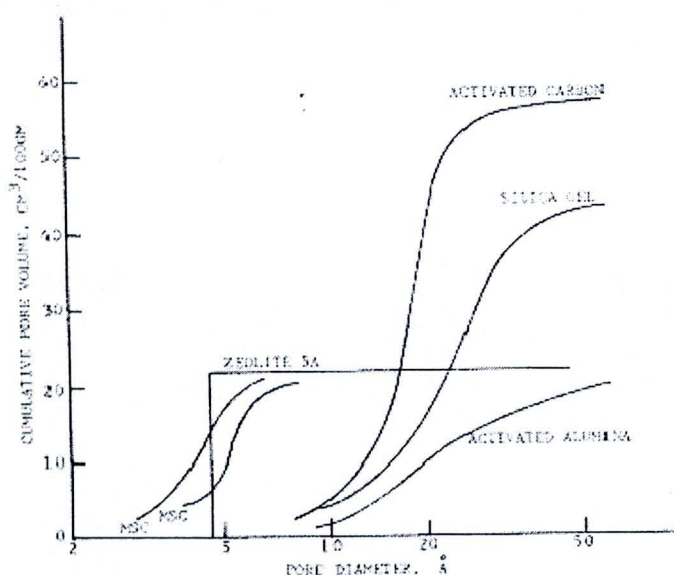
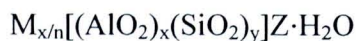


Figure 2.3 Pore-size distribution for activated carbon, silica gel, activated alumina, two molecular-sieve carbons, and zeolite 5A.

2.2.2 Zeolites

Zeolites are crystalline aluminosilicates of alkali or alkali earth elements such as sodium, potassium, and calcium, represented by the stoichiometry:



Where x and y are integers with y/x equal to or greater than 1, n is the valence of cation M , and Z is the number of water molecules in each unit cell. Unit cells are shown in Figure 2.6(b) and (c). The cations are necessary to balance the electrical charge of the aluminum atoms, each having a net charge of -1. The water molecules can be removed with ease upon heat and evacuation, leaving an almost unaltered aluminosilicate skeleton with a void fraction between 0.2 and 0.5. The skeleton has a regular structure of cages, which are usually interconnected by six windows in each cage. The cages can imbibe or occlude large amounts of guest molecules in place of water. The size of the window apertures, which can be controlled by fixing the type and number of cations, ranges from 3 Å to 10 Å. The sorption may occur with great selectivity because of the size of the aperture (and to a lesser extent because of the surface property in the cages) – hence the name *molecule sieve*.

At least forty species of naturally occurring zeolites have been found. The principal ones are chabazite, $(Ca, Na_2)Al_2Si_4O_{12}(6H_2O)$; gmelinite, $(Na_2, Ca)Al_2Si_4O_{12}(6H_2O)$; modenite, $(Ca, K_2, Na_2), Al_2Si_{10}O_{24}(6.66H_2O)$; levynite, $CaAl_2Si_3O_{10}(5H_2O)$; and faujasite, $(Na_2, Ca, Mg, K_2)OAl_2Si_{4.5}O_{12}(7H_2O)$. More than 150 types of zeolites have been synthesized; they are designated by a letter or group of letters – Type A, Type X, Type Y, Type ZSM, and so on. The commercial production of synthetic zeolites started with the successful development of low-temperature (25-100°C) synthesis methods using very reactive materials such as freshly coprecipitated gels or amorphous solids. Two comprehensive monographs, by Barrer and Breck, deal with all aspects of zeolites.

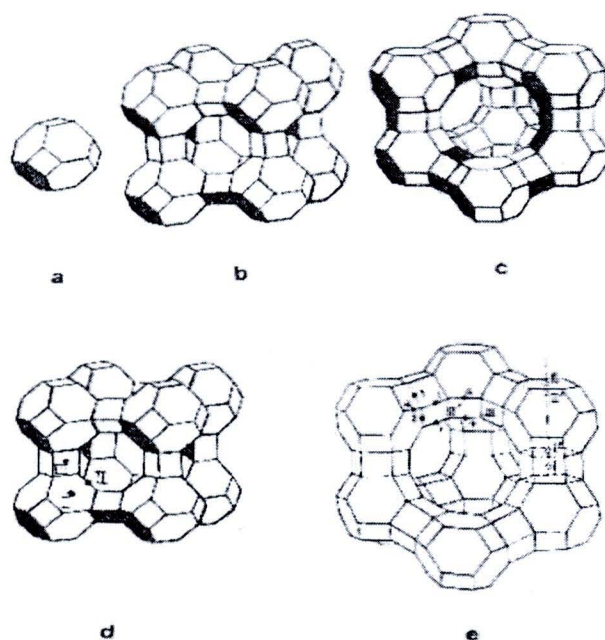


Figure 2.4 Line representation of zeolite structure: (a) sodalite cage, or truncated octahedron; (b) type A zeolite “unit cell”; (c) “unit cell” of types X and Y, or faugjasite; (d) cation sites in type A (there are eight I, three II, and twelve II sites per unit cell; (e) cation sites in types X and Y (16 I, 32 I', 32 II', 48 III, and 32 III' sites per unit cell).

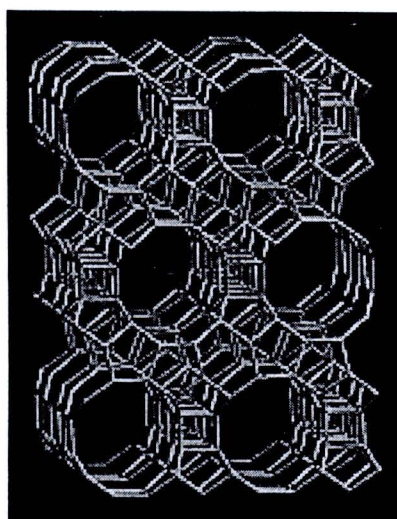


Figure 2.5 Structure of beta zeolite



Structures and Cation Sites

The primary structural units of zeolites are the tetrahedral of silicon and aluminum, SiO_4 and AlO_4 . These units are assembled into secondary polyhedral building units such as cubes, hexagonal prisms, octahedral, and truncated octahedral. The silicon and aluminum atoms, located at the corners of the polyhedral, are joined by a shared oxygen. The final zeolite structure consists of assemblages of the secondary units in a regular three-dimensional crystalline framework. The ratio Si/Al is commonly one to five. The aluminum atom can be removed and replaced by silicon in some zeolites, thereby reducing the number of cations; and the cations can also be exchanged. The inner atoms in the windows are oxygen. The size of the windows depends, then, on the number of oxygen atoms in the ring – four, five, six, eight, ten, or twelve. The aperture size, as well as the adsorptive properties, can be further modified by the number and type of exchanged cations. A description of the structures will be given only for the zeolites important in gas separation, Type A and Types X and Y.

Zeolite A The structural unit in Type A zeolite, as well as in Types X and Y, is the truncated octahedron, shown in Figure 2.4(a). This unit is also called sodalite cage, as sodalite is formed by directly fusing the four-member rings of the units. The four-member rings of the sodalite units can also be linked through four-member rings of the units. The four-member rings of the sodalite units can also be linked through four-member rings of the units. The four-member rings of the sodalite units can also be linked through four-member prisms, as shown in Figure 2.4(b), which is Type A zeolite. The unit cell of Type A zeolite, as shown in this figure, contains 24 tetrahedral, 12 AlO_4 and 12 SiO_4 . When fully hydrated, 27 water molecules are contained in the central cage or cavity of the unit cell, and in the eight smaller sodalite cages. The free diameter in the central cavity is 11.4 Å, which is entered through six eight-member oxygen-ring apertures with a minimum diameter of 4.4 Å. There are twelve negative charges to be balanced by cations in each unit cell. The most probable locations for the cations are indicated in Figure 2.4(d). Type I is at the center of the six-member ring, thus at one of the eight corners of the cavity. Type II is at the eight-member aperture, directly obstructing the entrance. Type III is near the four-member ring inside the cavity. Type A zeolites are synthesized in the sodium form, with 12 sodium cations occupying all eight

sites in I and three sites in II, plus one site in III. This is the commercial Type 4A zeolite, with an effective aperture size of 3.8 Å. The sodium form can be replaced by various other cations or by a hydrogen ion. The commercial Type 3A zeolite is formed by exchanging Na⁺ with K⁺, resulting in a smaller effective aperture size due to the large K⁺. The aperture size of the sodium form can also be increased by exchanging Na⁺ with Ca⁺² or Mg⁺², since 2 Na⁺ are replaced by one bivalent cation. The form of the exchanged Ca⁺² or Mg⁺² is Type 5A with rather unobstructed and larger apertures.

Framework

Space Group:	Pm-3m	
Cell Parameters:		
$a = 11.919 \text{ \AA}$	$b = 11.919 \text{ \AA}$	$c = 11.919 \text{ \AA}$
$\alpha = 90.000^\circ$	$\beta = 90.000^\circ$	$\gamma = 90.000^\circ$
Volume =	1693.24 Å ³	
R _{DLS} =	0.0026	
Framework density	14.2 T/1000 Å ³	
(FD_{Si}):		
Topological density:	TD ₁₀ = 641	TD = 0.533333
Ring sizes (# T-atoms)	8 6 4	
Channel system:	3-dimensional	
Secondary Building Units:	8 or 4-4 or 6-2 or 6 or 1-4-1 or 4	

Source : International Zeolite Association (IZA)

Zeolite X and Y The skeletal structure of Types X and Y zeolites is the same as that of the naturally occurring faujasite. The sodalite units are linked through six-member prisms, as shown in the unit cell in Figure 2.4(c). Each unit cell contains 192 (Si,Al)O₄ tetrahedral. The number of aluminum ions per unit cell varies from 96 to 77 for Type X zeolite, and from 76 to 48 for Type Y zeolite. This framework has the largest central cavity volume of any known zeolite, amounting to about 50% void fraction in the dehydrated form. A unit cell, when fully hydrated, contains approximately 235 water

molecules, mostly in the supercage, The aperture is formed by the twelve-member oxygen rings with a free diameter of approximately 7.4 Å. Three major locations for the cations are indicated in Figure 2.6(e). The locations are: center of the six-member prism (I) and opposite to I in the sodalite cage (I'); similar to I and I' but further from the central cavity (II and II'); and at the twelve-member aperture (III and III'). The commercial 10X zeolite contains Ca^{+2} as the major cation, and Na^{+} is the major cation for 13X zeolite. The distribution of Na^{+} , K^{+} , Ca^{+2} , other cations and H_2O in X and Y zeolites among the sites have been discussed in detail by Barrer. The BET surface area measured with N_2 for zeolites falls in the range between 500 and 800 m^2/g [6].

Framework

Space Group: Fd-3m (origin choice 2)

Cell Parameters:

$a = 24.345 \text{ Å}$ $b = 24.345 \text{ Å}$ $c = 24.345 \text{ Å}$

$\alpha = 90.000^\circ$ $\beta = 90.000^\circ$ $\gamma = 90.000^\circ$

Volume = 14428.77 Å^3

$R_{\text{DLS}} = 0.0009$

Framework density 13.3 T/1000 Å^3

(FD_{Si}):

Topological density: $\text{TD}_{10} = 579$ $\text{TD} = 0.476190$

Ring sizes (# T-atoms) 12 6 4

Channel system: 3-dimensional

Secondary Building Units: 6-6 or 6-2 or 6 or 4-2 or 1-4-1 or 4

Source : International Zeolite Association (IZA).

Beta zeolite Crystallographic faulting in zeolite structures affects both the catalytic and sorption properties, and can greatly complicate attempts at structural characterization. A near extreme example of stacking disorder is provided by zeolite beta, a large pore, high-silica zeolite that was first reported in 1967. Zeolite beta can be regarded as a highly intergrown hybrid of two distinct, but closely related structures that

both have fully three-dimensional pore systems with 12-rings as the minimum constricting apertures. One end member, polymorph A, forms an enantiomorphic pair, space group symmetries $P4_122$ and $P4_322$, with $a = 1.25$ nm, $c = 2.66$ nm. Polymorph B is achiral, space group $C2/c$ with $a = 1.76$ nm, $b = 1.78$ nm, $c = 1.44$ nm, $\beta = 114.5$ circ. Both structures are constructed from the same centrosymmetric tertiary building unit (TBU), arranged in layers that, successively, interconnect in either a left- (L) or a right- (R) handed fashion. Polymorph A represents an uninterrupted sequence of RRRR... (or LLLL...) stacking. Polymorph B has an alternating RLRL... stacking sequence. The TBU has no intrinsic preference for either mode of connection, enabling both to occur with almost equal probability in zeolite beta, giving rise to a near random extent of interplanar stacking faults and, to a lesser extent, intraplanar defects terminated by hydroxyl groups. The faulting does not significantly affect the accessible pore volume, but influences the tortuosity of the pore connectivity along the c direction. The high stacking fault densities give rise to complex powder X-ray diffraction (PXD) patterns for zeolite beta materials that comprise both sharp and broad features. By exploiting recursive relations between possible stacking sequences, PXD patterns have been calculated as a function of faulting probability. Reasonable agreement with observed PXD profiles is observed for a 60% faulting probability in the chiral stacking sequence, suggesting a slight preference for polymorph B. The framework building units observed in zeolite beta can also be used to construct other frameworks [7].

Framework

Space Group:	P4 ₁ 22		
Cell Parameters:			
$a = 12.632 \text{ \AA}$	$b = 12.632 \text{ \AA}$	$c = 26.186 \text{ \AA}$	
$\alpha = 90.000^\circ$	$\beta = 90.000^\circ$	$\gamma = 90.000^\circ$	
Volume =	4178.43 \AA^3		
R _{DLS} =	0.0022		
Framework density			
(FD_{Si}):	15.3 T/1000 \AA^3		

Topological density: $TD_{10} = 805$ $TD = 0.704545$

Ring sizes (# T-atoms) 12 6 5 4

Channel system: 3-dimensional

Secondary Building Units: combinations only

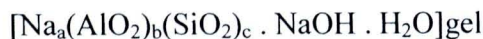
Source : International Zeolite Association (IZA)

Manufacture Procedure and Applications for Gas Separation

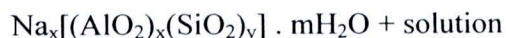
Commercial zeolite pellets are made in the following sequence: synthesis, palletizing, and calcination. Many alkali metal hydroxides and raw materials containing silica and alumina can be used in low-temperature synthesis. The steps involving the $\text{Na}_2\text{O}-\text{Al}_2\text{O}_3-\text{SiO}_2-\text{H}_2\text{O}$ system, which is used in synthesizing zeolites of types A, X and Y, are as follows;



$T_1 \approx 25^\circ\text{C}$



$T_2 \approx 25-175^\circ\text{C}$



The first step involves gel formation between sodium hydroxide, sodium silicate, and sodium aluminate in aqueous solution at room temperature. The gel is probably formed by the copolymerization of the silicate and aluminate species by a condensation-polymerization mechanism. Expressed in mole per mole of Al_2O_3 for $\text{Na}_2\text{O}/\text{SiO}_2/\text{H}_2\text{O}$, the compositions of the reactants are:

1. Type 4A zeolite, 2/2/35
2. Type X zeolite, 3.6/3/144
3. Type Y zeolite, 8/20/320



The gels are crystallized in a closed hydrothermal system at temperatures between 25°C and 175°C. Higher temperatures upto 300°C are used in some cases. The time for crystallization ranges from a few hours to several days.

The crystals formed are cubic single crystals with sizes ranging from 1 to 10 microns. For example, the commercial 5A zeolite contains cubic crystals with a mean size slightly greater than 2 microns. (The largest crystal synthesized is near 100 microns.) Types 3A and 5A zeolites are formed by ion exchange in the crystallization step by adding aqueous solutions of potassium and calcium salts, respectively. The crystals, after calcination at about 600°C, are further agglomerated and palletized with or without a binder amounting to less than 20% of the pellets. The binder has a negligibly small capacity for the adsorption of gases. The characteristics of the major commercial zeolite sorbents in the palletized forms are given in Table 2.2.

Table 2.2 Characteristic of major synthetic zeolite sorbents.

Zeolite type	Major cation	Nominal aperture size, Å	Bulk density^a, lb/ft³	Water^b capacity, wt%
3A (Linde)	K	3	40	20.0
3A (Davidson)	K	3	46	21.0
4A (Linde)	Na	4	41	22.0
4A (Davidson)	Na	4	44	23.0
5A (Linde)	Ca	5	45	21.5
5A (Davidson)	Ca	5	44	21.7
10X (Linde)	Ca	8	40	31.6
13X (Linde)	Na	10	38	28.5
13X (Davidson)	Na	10	43	29.5
Beta (Zeochem)	Na	7.6x6.4 / 5.5x5.5	-	-

^aBased on 1/16 inch pellets or beads.

^bThe dried sorbent contains < 1.5 weight-percent water in Linde products and 1.5 weight-percent in Davidson products.

In Table 2.3, important industrial gases are grouped according to their molecular sizes, which are smaller than the apertures of the zeolite types, and hence can be adsorbed. In principle, any mixture containing gases from different groups can be separated by molecular sieving. Many of the important zeolite-based gas separation processes currently practiced in industry, however, are not based on molecular-sieving action. They are based on the different equilibrium amounts adsorbed, of the constituents in the mixture. The important gas separation processes using zeolite sorbents are: air

n-paraffins from branched-chain and cyclic hydrocarbons, aromatic hydrocarbon separation, and drying. Except for the n-paraffin and aromatics separations, these processes employ the preferential adsorption of certain components. For example, nitrogen is preferentially adsorbed over oxygen (by approximately threefold in 5A zeolite) as a result of its quadruple moment, which forms a strong bond with the polar surface.

2.2.3 Silica Gel

Silica gel is one of the synthetic amorphous silica. It is a rigid, continuous network of spherical particles of colloidal silica. There are a number of preparation methods, which result in different pore structures.

Manufacturing Procedure

Commercially, silica gel is prepared by mixing a sodium silicate solution with a mineral acid such as sulfuric or hydrochloric acid. The reaction produces a concentrated dispersion of finely divided particles of hydrated SiO_2 , known as silica hydrosol or silicic acid:



Table 2.3 Molecules Admitted to Zeolites According to Molecular Dimensions and Zeolite Aperture Sizes

Molecular size increasing →

He, Ne, Ar, CO H ₂ , O ₂ , N ₂ , NH ₃ , H ₂ O Size limit for Ca- and Ba- mordenites and levynite about here (≈ 3.8 Å)	Kr, Xe CH ₄ C ₂ H ₆ CH ₃ OH CH ₃ CN CH ₃ NH ₂ CH ₃ Cl CH ₃ Br CO ₂ C ₂ H ₂ CS ₂ Size limit for Na- mordenite and Linde sieve 4A about here (≈ 4.0 Å)	C ₃ H ₈ n-C ₄ H ₁₀ n-C ₇ H ₁₆ n-C ₁₄ H ₃₀ etc. C ₂ H ₅ Cl C ₂ H ₅ Br C ₂ H ₅ OH C ₂ H ₅ NH ₂ CH ₂ Cl ₂ CH ₂ Br ₂ CHF ₂ Cl CHF ₃ (CH ₃) ₂ NH CH ₃ I B ₃ H ₆ Size limit for Ca-rich chabazite, Linde sieve 5A, Ba-zeolite and gmelinite about here (≈ 4.9 Å)	C ₂ F ₆ CF ₂ Cl ₂ CF ₃ Cl CHFCl ₂	SF ₆ iso-C ₄ H ₁₀ iso-C ₃ H ₁₂ iso-C ₄ H ₁₈ etc. CHCl ₃ CHBr ₃ CHI ₃ (CH ₃) ₂ CHOH (CH ₃) ₂ CHCl n-C ₄ F ₈ n-C ₄ F ₁₀ n-C ₇ F ₁₆ B ₃ H ₉	(CH ₃) ₃ N (C ₂ H ₅) ₃ N C(CH ₃) ₄ C(CH ₃) ₃ Cl C(CH ₃) ₃ Br C(CH ₃) ₃ OH CCl ₄ CBr ₄ C ₂ F ₂ Cl ₄	C ₆ H ₆ C ₆ H ₅ CH ₃ C ₆ H ₄ (CH ₃) ₂ Cyclopentane Cyclohexane Thiophene Furan Pyridine Dioxane B ₁₀ H ₁₄	Naphthalene Quinoline, 6-decyl-1, 2, 3, 4-tetra- hydro- naphthalene, 2-butyl-1- hexyl indan C ₆ F ₁₁ CF ₃	1, 3, 5-triethyl benzene 1, 2, 3, 4, 5, 6, 7, 8, 13, 14, 15, 16-decahydro- chrysene	(n-C ₃ F ₉) ₃ N
Type 5	Size limit for Ca-rich chabazite, Linde sieve 5A, Ba-zeolite and gmelinite about here (≈ 4.9 Å)				Size limit for Linde sieve 10X about here				
Type 4					Size limit for Linde sieve 13X about here (≈ 10 Å)				
Type 3									
Type 2									
Type 1									

The hydrosol, on standing, polymerizes into a white jellylike precipitate, which is silica gel. The resulting gel is washed, dried and activated. Various silica gels with a wide range of properties such as surface area, pore volume and strength can be made by varying the silica concentration, temperature, pH and activation temperature. Two typical types of silica gel are known as regular-density and low-density silica gels, although they have the same densities (true and bulk). The regular-density gel has a surface area of 750-850 m²/g and an average pore diameter of 22-26 Å, whereas the respective values for the low-density gel are 300-350m²/g and 100-150 Å. The micropore volume of the regular-density gel is shown in Figure 2.3.

Silica gel, along with activated alumina, is a desirable sorbent for drying because of its high surface areas and unique surface properties. Silica gel contains 4-6% "water" by weight, which is the measured "loss on ignition." This so-called water is essentially a monolayer of hydroxyl groups bound to the silicon atoms on the surface, forming the silanol, Si-O-H, groups. The surface chemistry of silica gel has been extensively studied by infrared and near-infrared spectroscopic techniques, as it is a good infrared window and hence suitable for these techniques. Some of these studies on the interaction of water on silicas were reviewed by Klier and Zettlemoyer. At a low surface coverage, evidence shows that the water molecule is bound to the silanol group "oxygen down"



At higher coverages, hydrogen bonding within clusters of water becomes predominant, with a bond strength or heat of adsorption approaching of water vapor on silica gel is approximately 11 kcal/mole --- essentially the same as that on activated alumina. The relatively low heat of adsorption and consequently, weakly held water are desirable for sorbent regeneration. Regeneration of silica gel is achieved by heating to approximately 150°C, as compared to 350°C for zeolites, where the heats of adsorption of water vapor are considerable higher. A lower heat of adsorption is also desirable in separation processes because the temperature rise resulting from adsorption lowers the adsorption capacity, and a detrimental temperature drop occurs during desorption or regeneration. (Zeolites, however, the advantage of higher water capacities at low relative pressures; hence they are used at high temperatures.)

The equilibrium water sorption capacity at 25°C for the regular-density gel is shown in Figure 2.2. The water capacity for the low-density gel is substantially lower.

2.2.4 Activated Alumina

Activated alumina is one of the solids having the greatest affinity for water. An important industrial application for activated alumina continues to be the drying of gases and liquids, because of its hydrophilic property and large surface area. The term activated alumina refers to dehydrated or partially dehydrated alumina hydrates, both crystalline and amorphous, with high surface areas. It has been prepared by a variety of procedures.

Manufacturing Procedures and Surface Areas

Commercial production is exclusively by thermal dehydration or activation of aluminum trihydrate, $\text{Al}(\text{OH})_3$ or gibbsite. The oldest form, which is still widely used, is made from Bayer α -trihydrate, which is a by-product of the Bayer process for aqueous caustic extraction of alumina from bauxite. The trihydrate, in the form of gibbsite, is heated or activated in air to about 400°C to form crystalline γ/η -alumina with a minor amount of boehmite, and has a surface area of approximately 250 m²/g. Alternatively, the trihydrate is heated very rapidly at 400-800°C to form an amorphous alumina with a higher surface area, 300-350 m²/g. The major impurity in these products, besides water (typically 6%), is Na_2O at nearly 1%. The micropore volume is shown in Figure 2.3, but there is a considerable number of pores with sizes greater than 50 Å. A highly impure form of activated alumina is made by the thermal activation of bauxite, which contains alumina in the form of gibbsite.

Adsorption Applications

The major use of activated alumina as a sorbent is in drying. It also finds application in chromatography. A partial list of industrial gases that can be dried by activated alumina includes: Ar, He, H_2 , low alkanes (mainly C1-C3) and hydrocarbons, Cl_2 , HCl, SO_2 , NH_3 , and Freon fluorochloralkanes. It has been especially important in the drying of hydrocarbons produced by the thermal cracking of petroleum fractions. It, however, suffers a loss of adsorption capacity with prolonged use as a result of coking

and contamination. This is a common problem for all sorbents. The moisture content can be reduced to below 1 ppm using activated alumina in suitable designed adsorbers.

2.3 Selection of Sorbent

The selection of a proper sorbent for a given separation is a complex problem. The predominant scientific basis for sorbent selection is the equilibrium isotherm. The equilibrium isotherms of all constituents in the gas mixture, in the pressure and temperature range of operation, must be considered. As a first and possibly oversimplified approximation, the pure-gas isotherms may be considered additive to yield the adsorption from a mixture. Based on the isotherms, the following factors that are important to the design of the separation process can be estimated:

1. Capacity of the sorbent, in the operating temperature and pressure range.
2. The method of sorbent regeneration – for example, thermal or pressure swing and the magnitude of the required swing.
3. The length of the unusable (or unused) bed (LUB).
4. The product purities.

The LUB is approximately one-half of the span of the concentration wavefront, or the mass transfer zone. The LUB is primarily determined by the equilibrium isotherm. A sharp concentration front, or a short LUB, is desired because it results in a high sorbent productivity as well as a high product purity.

Consideration should also be given to other factors. As mentioned, activated carbon is the only commercial sorbent used for wet gas stream processing. (A predryer is required for other sorbents.) Sorbent deactivation, primarily by coke deposition, is an important consideration in the processing of hydrocarbon containing gases. Coke is formed catalytically, and zeolites are excellent catalysts for these reactions. Pore-size distribution can play a role in the LUB, but not as importance role as that of the equilibrium isotherm, since the commercial sorbent pellets are designed to minimize the pore-diffusion resistance. Kinetic separation that is, separation based on the difference between pore diffusivities of two gases has found only one application: the production of

nitrogen from air by molecular sieve carbon. Dehydration of cracked gases with 3A zeolite and the separation of normal and iso-paraffins with 5A zeolite are based on selective molecular exclusion. All other commercial processes are based on the equilibrium isotherms. Temperature for activation and regeneration of the sorbent should also be considered. A high temperature of nearly 300°C is required for zeolites, whereas activated carbon usually requires the lowest temperature for regeneration.

The total void space in the bed, which varies with the sorbents, is also an important factor. A low void space is desired for high product recoveries since the gas mixture remaining the void space in the saturated bed is usually not recovered as a useful product. Silica gel and activated alumina have the lowest void fraction, usually slightly below 70%; activated carbon has the highest void fraction, at nearly 80%.

2.4 Effect of molecular sieve on adsorption

Molecular sieving by dehydrated zeolite crystals is caused by the size and/or shape differences between the crystal aperture and the adsorbate molecule [14].

In order to correlate the crystallographic aperture or pore size of a zeolite with the dimensional parameters of various adsorbate molecules, a scale of molecular dimensions was established. In early experiments, the molecular size was based upon the equilibrium diameter of the adsorbate molecule. This was arrived at by calculation using the known molecular shape, bond distances, bond angles, and van der Waals radii. It was observed that certain molecules were freely adsorbed but were larger than the known aperture size of the zeolite crystal. In an improved treatment of this problem, Kington and MacLeod have utilized the collision or kinetic diameter.

The effective pore size of a zeolite molecular sieve can be determined from the sizes of molecules which are or are not adsorbed under a given set of conditions. For example, at temperatures of -183 to -196°C, zeolite A adsorbs oxygen freely while nitrogen is not adsorbed over long periods of time. At these temperatures, nitrogen diffusion is so slow that true equilibrium cannot be attained.



The Kinetic Diameter

For spherical and nonpolar molecules the potential energy of interaction, $\phi(r)$ is well described by the Lennard-Jones potential

$$\phi(r) = 4\epsilon \left[\left(\frac{\sigma}{r} \right)^{12} - \left(\frac{\sigma}{r} \right)^6 \right]$$

The parameters, σ and ϵ , are constants which are characteristic of the molecular species and are determined from second virial coefficients. At large separations the attractive component, $(\sigma/r)^6$, is dominant and describes the induced dipole-induced dipole interaction. At small separations the repulsive component is dominant (Fig. 2.5). When the potential equals 0 the diameter, r , is equal to σ . The *kinetic* or collision diameter is the intermolecular distance of closest approach for two molecules colliding with zero initial kinetic energy. The maximum energy of attraction, ϵ , occurs at r_{\min} , where $r_{\min} = 2^{1/6} \sigma$.

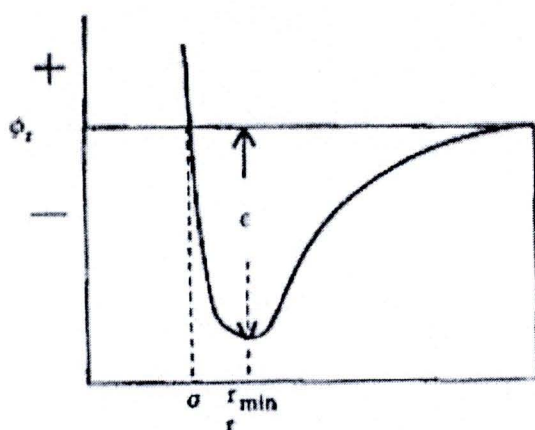


Figure 2.6 Relationship between equilibrium diameter, r_{\min} and kinetic diameter, σ .
 $r_{\min} = 2^{1/6} \sigma$.

In assessing the apparent pore size of molecular sieve zeolites, the critical dimensions for spherical molecules are given by the value of r_{\min} . For diatomic molecules, r_{\min} is based upon the van der Waals length, and represents the molecule in all orientations. For long molecules, such as hydrocarbons, the dimension is the minimum cross-sectional diameter. It is preferred to use σ values obtained from minimum cross-sectional diameters for more complex molecules, such as n-paraffins.

For polar molecules, the Stockmayer potential function is widely used for describing the interaction between molecules for which dipole-quadrupole interactions are not important. Values of the parameter σ determined for certain polar molecules have been used. Kihara's data were used for spherocylindrical and ellipsoidal molecules (H_2 and N_2).

Table 2.4 lists molecular dimensions calculated from Pauling along with r_{\min} and σ , the minimum kinetic diameter. For complex molecules, the minimum equilibrium diameter of Pauling was used to compute σ . Adsorption phenomena indicate that the minimum equilibrium diameter should be used as r_{\min} in computing σ . For example, the Lennard-Jones approach gives a value of $\sigma = 4.05$ for CO_2 and 3.64 for N_2 . Under equivalent conditions, KA adsorbs CO_2 but not N_2 . Therefore, the minimum equilibrium dimension of 3.7 Å was used to compute a σ value of 3.3 Å. The σ values for H_2O and NH_3 were obtained from data given by the Stockmayer potential.

Figure 2.6 compares σ , the minimum kinetic diameter, with the apparent pore diameter of various zeolites. Calcium A has a pore diameter of 4.2 Å as determined by structural analysis. This compares well with the σ value of 4.3 for n-paraffins and 4.4 Å for CF_2Cl_2 which is adsorbed at about 150°C. Thus, the apparent pore size of CaA varies from 4.2-4.4 Å. NaA adsorbs C_2H_4 (slowly) and CH_4 , $\sigma = 3.9$ and 3.8 Å, respectively. At low temperatures, it does not adsorb N_2 . The apparent pore diameter is 3.6 to 4.0 Å, depending on temperature. The explanation for this variation has been based upon a process of activated diffusion. It has also been postulated that thermal vibration of the oxygen ions, and cations, in the zeolite lattice surrounding the apertures is responsible [14].

Table 2.4 Dimensions for various molecules.

	Pauling	<i>Lennard-Jones</i>		
	length (Å)	Width (Å)	<i>r</i> min (Å)	σ (Å) ^a
He		~ 3	3.0	2.6
H ₂	3.1	2.4	3.24	2.89
Ne		3.2	3.08	2.75
Ar		3.84	3.84	3.4
O ₂	3.9	2.8	4.02	3.46
N ₂	4.1	3	4.09	3.64
Kr		3.96	3.96	3.6
Xe		4.36	4.45	3.96
NO	4.05	3	3.58	3.17
N ₂ O	4.2	3.7		3.3
CO	4.2	3.7	4.25	3.76
CO ₂	5.1	3.7		3.3
Cl ₂	5.6	3.6		3.2
Br ₂	6.2	3.9		3.5
H ₂ O	3.9	3.15		2.65
NH ₃	4.1	3.8		2.6
SO ₂	5.28	4		3.6
CH ₄		4.2	4.25	3.8
C ₂ H ₂	5.7	3.7	3.7	3.3
C ₂ H ₄	5	4.4		3.9
C ₃ H ₈	6.5	4.9		4.3
n-C ₄ H ₁₀		4.9		4.3
HCl	4.29	3.6		3.2
HBr	4.6	3.9		3.5
H ₂ S	4.36	4		3.6
CS ₂		4		3.6
CF ₂ Cl ₂		5		4.4
CCl ₄			6.65	5.9

	Pauling	Lennard-Jones	
	length (Å)	Width (Å)	σ (Å) ^a
iso-C ₄ H ₁₀		5.6	5
Butene-1			5.1
CF ₄		4.9	5.28
SF ₆		5.8	6.18
Neopentane		7	
(C ₄ H ₉) ₃ N			9.1
(C ₂ F ₅) ₂ NC ₃ F ₇		8.7	
(C ₄ F ₉) ₃ N		11.5	
Benzene		6.6	
(C ₂ H ₅) ₃ N			8.8
Cyclohexane		6.7	6

^a Kinetic diameter, σ calculated from the minimum equilibrium cross-sectional diameter.



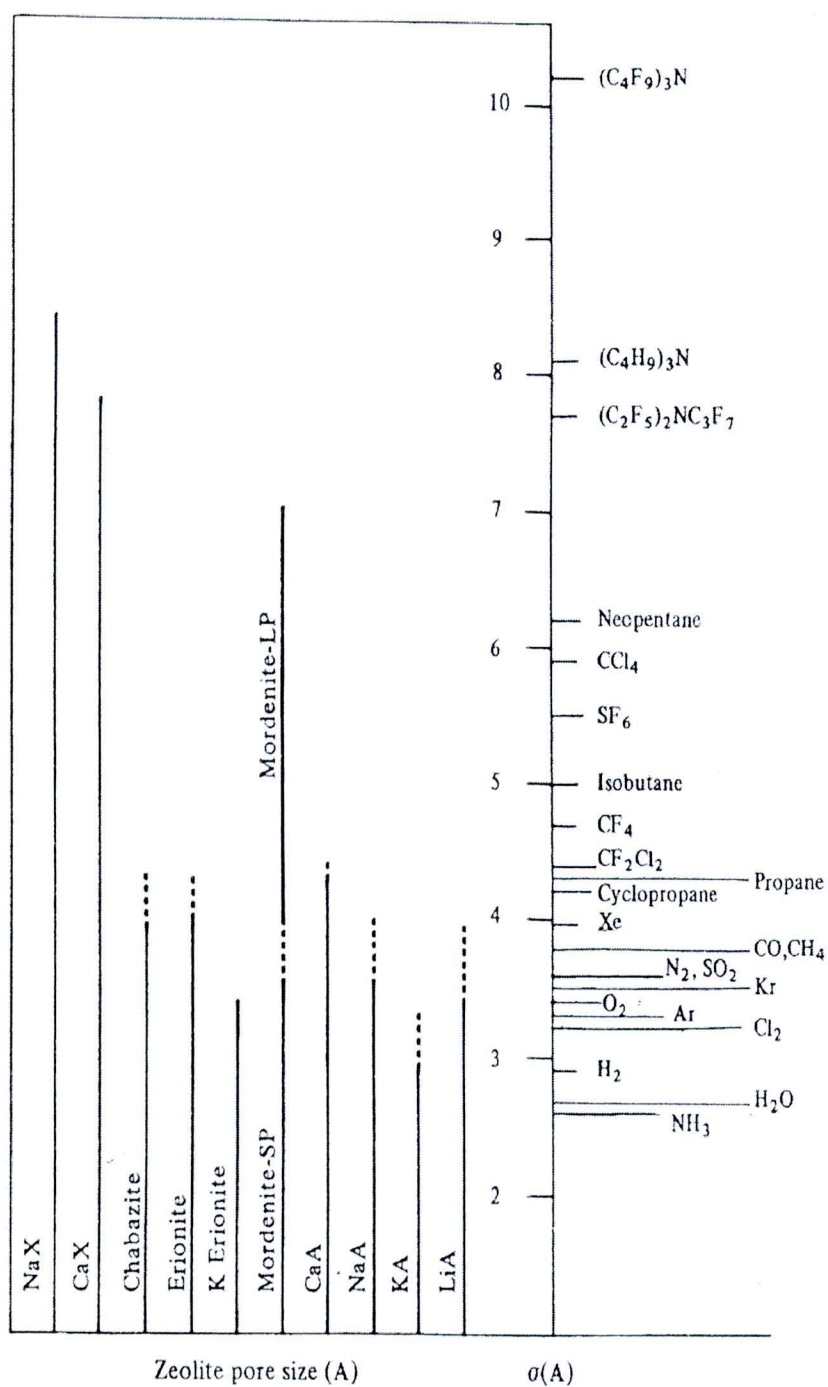


Figure 2.7 Chart showing a correlation between effective pore size of various zeolites in equilibrium adsorption over temperatures of 77° to 420°K (indicated by - - -), with the kinetic diameters of various molecules as determined from the L-J potential relation.

2.5 Literature Review

In 2008, Thiti L. and Tharapong V. studied suitable condition for separation of moisture from ethanol in gas phase by zeolite 3A and 4A at atmosphere. The ratio of zeolite 3A and 4A was investigated. The feed gas is 95%wt EtOH in moisture. They found that 100% of 3A provides the best result. The suitable condition is 90°C, flowrates 1 ml/min [11].

In 2006, Peiyuan Li and F. Handan Tezel studied adsorption equilibrium and kinetic separation potential of β -zeolite for N_2 , O_2 , CO_2 and CH_4 gases by using concentration pulse chromatography. With β -zeolite, CO_2 has the highest adsorption, followed by CH_4 , N_2 and O_2 . CO_2 separation from O_2 , N_2 and CH_4 has good equilibrium separation factors. This factor is not very high for CH_4/N_2 and CH_4/O_2 systems and is the lowest for N_2/O_2 system. With β -zeolite, the kinetic separation factors are very small at high temperatures for all the systems studied. N_2/CO_2 and O_2/CO_2 can be separated in kinetic processes with reasonable separation factors at temperatures lower than 31.9°C. Both equilibrium and kinetic separation factors decrease as column temperature increases [8].

In 2006, Simone Cavenati and colleagues studied adsorption-based process for removal of carbon dioxide and nitrogen from low and medium natural gas flowrates. The layered pressure swing adsorption (LPSA) process studied is composed of a zeolite 13X followed by a layer of carbon molecular sieve 3K. Experiments were performed in a single-column LPSA unit. The effect of temperature and ratios of adsorbent layer were studied. The feed gas is 60% CH_4 /20% CO_2 /20% N_2 . CH_4 purity of 86.0% with 52.6% recovery was obtained at ambient temperature while 88.8% purity with 66.2% recovery was obtained at 323 K. At both temperatures there was a ratio of adsorbent layers where purity reaches a maximum, while product recovery always decreases for larger zeolite 13X layers [13].

In 2005, José A. Delgado and colleagues studied the adsorption equilibrium isotherms of CO_2 , CH_4 and N_2 on Na- and H-mordenite at three temperatures (279, 293 and 308 K) for pressures up to 2 MPa. For Na-mordenite, the selectivity order is: carbon

dioxide \gg methane $>$ nitrogen. The selectivity order is the same for H-mordenite. The selectivity ratio CO_2/CH_4 is smaller than CH_4/N_2 . The adsorption capacity for CH_4 and N_2 is recovered with vacuum in both adsorbents, whereas this does not apply to CO_2 for Na-mordenite [16].

In 1999, S. E. Iyuke and colleagues studied Sn-activated carbon (Sn-AC) in pressure swing adsorption (PSA) system in the purification of hydrogen for PEM fuel cell application. Activated carbon was impregnated with 34.57% $\text{SnCl}_2 \cdot 2\text{H}_2\text{O}$ salt and then dried to produce AC- SnO_2 to improve its adsorptive interaction with CO. The concentration of CO, which was 1000 ppm, was reduced to 40.2 and 10.4 ppm by the pure and the impregnated activated carbons, respectively. The use of AC- SnO_2 in adsorbing CO proved superior to that when pure carbon was used for H_2 purification in a PSA system [10].

In 1991, Shang-Bin Liu and colleagues studied the thermal stability of zeolite beta by ^{129}Xe NMR and adsorption isotherm of adsorbed xenon in correlation with data from X-ray diffraction and ^{27}Al magic-angle-spinning NMR experiments. Samples subject to different calcination and dehydration conditions were examined. Minor destruction of the crystalline framework resulting from dealumination processes has been found for samples treated at a temperature 400°C [12].